

## CFD modelling of the velocity profile within a Single Horizontal Fracture in an Enhanced Geothermal System

Zhao Feng Tian<sup>1</sup>, Rosemarie Mohais<sup>2</sup>, Chaoshui Xu<sup>2</sup>, and Xiongwei Zhu<sup>1</sup>

<sup>1</sup>School of Mechanical Engineering

University of Adelaide, South Australia 5005, Australia

<sup>2</sup>School of Civil, Environmental and Mining Engineering

University of Adelaide, Adelaide, South Australia 5005, Australia

### Abstract

Accurate prediction of geothermal fluid velocity profiles in the fractures is essential in determining the mass flow rate and hence energy extraction in Enhanced Geothermal Systems (EGS) which embrace Hot Dry Rock (HDR) systems and Hot Sedimentary Aquifer (HAS) systems. Previous studies have addressed flows in fractures assuming fracture walls as impermeable boundaries. However this assumption is unrealistic since the channel walls may contain cracks and fissures arising from the initial hydraulic fracturing process. The channel walls thus exhibit permeable characteristics at the boundary which will affect the velocity profiles in the fracture. There has been recent development of mathematical models to predict velocity profiles for low Reynolds number flows in HDR fractures by considering the effects of slip boundary conditions at the walls. In this paper, computational fluid dynamics (CFD) model based on the Finite Volume approach is used to predict the fluid velocity profile in a single fracture in an EGS system. A fluid-porous interface model based on an analytical equation has been implemented in the commercial CFD code ANSYS/CFX. One advantage of this model is that it can take into consideration of different values of the slip coefficient,  $\alpha$ , which is a dimensionless quantity characterising the structure of permeable material at the fluid-porous interface wall. This interface velocity model is used to investigate the effects of values of  $\alpha$  on the channel flow. It is found when  $\alpha$  increases from 0.1 to 4, there is an increase in pressure drop in the flow. The fluid-porous interface velocity decreases and the maximum velocity at the center line of the channel increases as  $\alpha$  increases from 0.1 to 4.

### Introduction

Enhanced geothermal systems (EGS) are reservoirs created to extract energy from geothermal resources that are otherwise not economical due to lack of water and/or permeability [6]. The formation of this reservoir is based on the principle of heat extraction from hot dry rocks (HDR) located several kilometres below the surface [11]. These rocks are usually impermeable to flow in their natural state. Hydro-fracturing techniques are used by pumping pressurized water into the rock, resulting in the opening and propagation of existing fractures as well as the creation of new fractures to create a connected fracture network through which fluid can flow [11]. One of the important features of the geothermal reservoir is the efficiency, which is highly

dependent on the permeability through the rock fractures within the reservoir [12].

Many studies have been conducted on fluid flows in channels with porous walls over the last few decades. One of the significant contributions was provided by Beavers and Joseph [2]. They derived boundary conditions at naturally permeable wall for fully developed laminar flow by performing experiments of flow in a plane channel with solid upper wall and a lower porous wall [2]. They assumed that the volume-averaged flow in the core of the porous medium is governed by Darcy's Law [1],

$$0 = -\frac{dp}{dx} - \frac{\mu}{K}u \quad (1)$$

where  $p$  is the intrinsic volume-averaged pressure,  $x$  streamwise coordinate parallel to the channel,  $u$  the superficial volume-averaged velocity in  $x$  direction,  $\mu$  the dynamic viscosity, and  $K$  the permeability of the porous medium. The flow within the channel can be described using the Navier-Stokes (N-S) equations.

The solution from the N-S equations of a fully-developed laminar flow in a channel is a parabolic function for the velocity  $u$  in  $y$  direction ( $y$  is the lateral coordinate) along with an unknown velocity  $U_b$  at the interface. Beavers and Joseph [2] proposed the following boundary condition at the fluid-porous interface:

$$\frac{du}{dy} = \frac{\alpha}{\sqrt{K}}(U_b - Q) \quad (2)$$

where  $\alpha$  is the slip coefficient that is a dimensionless coefficient and  $Q$  is the filter velocity given by Darcy's Law (1). Based on the experimental data, Beavers and Joseph [2] could determine the value of the slip coefficient,  $\alpha$ , which ranged from 0.1 to 4 depending on the porous material (foametal or aloxite) that was used. Theoretical support for this was given by Saffman [13]. Saffman showed that the value of  $\alpha$  is sensitive to the definition of the location of the interface; this result was confirmed by the numerical simulations of Larson and Higdon [9][10]. Other similar numerical simulations showed that  $\alpha$  depends not only on the interfacial position, but also on the Reynolds number, filter velocity, the flow direction, the channel height, the porosity, and the surface topology [14].

Many researchers including Beavers and Joseph [2], Breugem, Boersma, and Uittenbogaard [4], Deng and Martinez [5] have

produced numerical solutions of the laminar flow with porous walls under different assumptions using either slip or non-slip wall boundaries. Berman [3] investigated the effect of wall porosity on the velocity and pressure distributions in a two-dimensional rectangular channel. He concluded that the velocity profile in the major flow direction is found to deviate from the Poiseuille parabola by being flatter at the centre of the channel and steeper in the region close to the walls, the degree of deviation depending on a Reynolds number for the flow through the channel walls. Granger, Dodds, and Midoux [8] published an analytical solution for the similar case without simplifying assumptions of constant permeation rate along the length of the Channel. They obtained the axial velocity profiles based on solving the Navier-Stokes equations. They concluded that the velocity profile is proportional to the ratio of the permeability to the thickness of the channel. In other words, the axial velocity profile differs from the classic parabolic shape. Mohais et al. [11] published detailed analysis results of velocity profile in a channel flow with permeable walls for an EGS. They confirmed that the axial flow profile is affected by slip boundary coefficient, permeability and the channel width for a channel with walls that contain small fissures, cracks and granular material.

This paper shows a computational fluid dynamics (CFD) model of fluid flows in a single horizontal fracture in an EGS system. The CFD model was developed using the commercial CFD package, ANSYS/CFX 14.0. This CFD package is based on the Finite Volume approach. The single fracture includes a fluid channel sandwiched by two porous domains. CFD models based on the Finite element approach have been developed and investigated previously, e.g. Tan and Pillai [15]. However, few papers have been found in modeling this kind of flows using Finite Volume approach. To better predict the velocity profiles, the analytical solution of Mohais et al. [11] was used to calculate the fluid velocity at the interface between the fluid and porous domains. One advantage of the analytical equation of Mohais et al. [11] is that it can take into consideration of the different values of the slip coefficient  $\alpha$ .

## Model formation

### Geometry and Mesh

ANSYS/Designmodeler was used to generate the CFD domains. A schematic diagram of the 2-dimensional (2D) numerical domain is given in Fig.1. The domain contains two sub-domains: the fluid domain and the porous domain. The height of the fluid flow channel is  $2h$ . As only half of the fracture is modelled in the CFD domain, symmetric boundary is used for the bottom boundary as shown in Fig. 1. The dimensions of the domains are listed in Table 1. Water is used as the fluid in both domains. Inlet velocities in the fluid channel of different cases were calculated based on Reynolds number of 0.5. The inlet of the porous domain has the same static pressure as the inlet of the fluid channel. Both outlets at the fluid and porous domains have the static pressure of 0 Pa. The porosity of the porous domain that is defined as the local ratio of the volume of fluid to the total physical volume is 20% in this study.

The mesh of the CFD domain is generated by using ANSYS/Meshing. The total number of mesh nodes is 486324 and the total element number is 240000. Figure 2 shows the mesh in the inlet region of the fluid domain and part of inlet region in the porous domain.

The laminar solver was used to solve the isothermal fluid flows under steady state. The convergence criteria were  $10^{-6}$  MAX.

Half channel height $h$ (m)	0.001
Porous medium height $b$ (m)	0.01
Channel length $L$ (m)	0.4

Table 1. Dimensions of CFD model used in CFX.

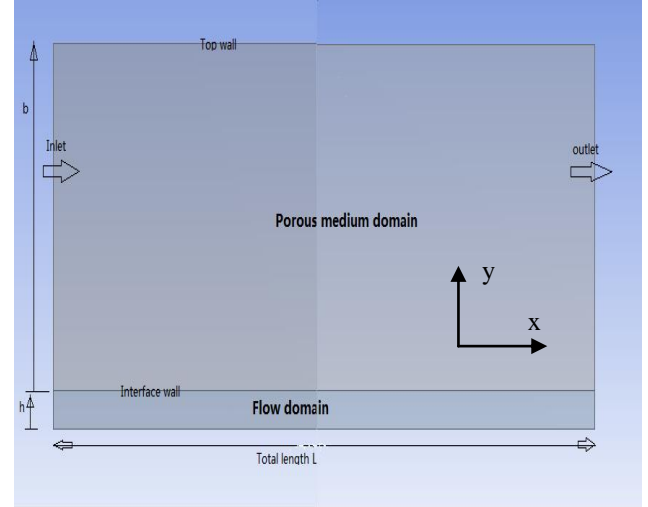


Fig.1. A truncated CFD model

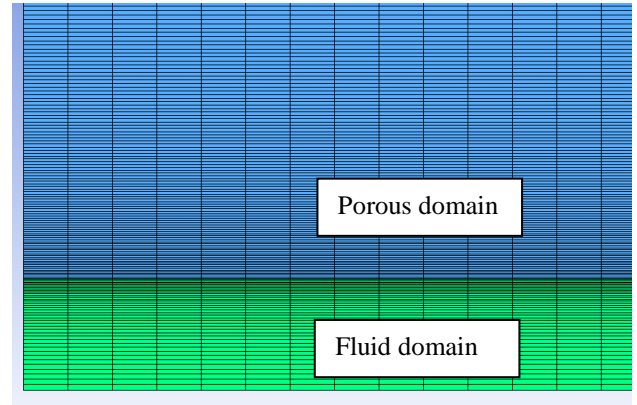


Fig.2. Computational grid at the inlet region.

### Interface boundaries

In this preliminary study, a no-slip wall boundary is used for the interface between the porous domain and the fluid domain. The fluid flow across the interface boundary is neglected. A velocity is imposed on the fluid-porous interface wall using the analytical equation developed by Mohais et al. [11]. The mathematical equations of these boundary conditions are given as below,

$$v_{\text{interface}} = 0 \quad (3)$$

$$u_{\text{interface}} = u_{\text{inlet}} f'(y^*) = u_{\text{inlet}} (f'_0(y^*) + \text{Re} f'_1(y^*)) \quad (4)$$

$$f_0(y^*) = y^{*3} \left( \frac{-1}{2(1+3\phi)} \right) + y^* \left( \frac{3+6\phi}{2+6\phi} \right) \quad (5)$$

$$f_1(y^*) = -\frac{y^{*7}}{2520} \left( \frac{9}{(1+3\phi)^2} \right) + \left( \frac{9(7\phi+1)}{140(1+3\phi)^3} \right) + y^* \left( \frac{1}{280(1+3\phi)^2} - \frac{3(7\phi+1)}{280(1+3\phi)^2} \right) \quad (6)$$

here  $\phi = \frac{\sqrt{K}}{\alpha h}$  and  $y^* = y/h$ .

At the fluid-porous interface wall,  $y^*$  has the value of 1. Results of four cases with  $\alpha = 0.1, 0.5, 1$  and  $4$ , respectively, are reported in this paper. The permeability of the porous media,  $K$ , is  $10^{-8} \text{ m}^2$ .

## Results and discussions

The predicted pressure drops through the computational domain of four cases are given in Table 2. As  $\alpha$  increases from 0.1 to 4, there is an increase in the pressure drop through the CFD domain. This is due to the decrease of the fluid velocity at the interface wall when  $\alpha$  increases (this will be discussed later). The decrease of interface velocity leads to higher pressure loss to overcome the higher wall stress.

$\alpha$	0.1	0.5	1	4
Pressure drop (Pa)	0.059	0.148	0.183	0.221

Table 2. Predicted pressure drop in different cases.

In the experimental study of Beavers and Joseph [2], Aloxite was tested and was found to have a minimum value of  $\alpha = 0.1$ . The velocity profiles at the outlet of the CFD model for the case of  $\alpha = 0.1$  is shown in Fig.3. Note that all velocities in the porous domain in the paper are superficial velocities. The  $x$ -axis is the axial velocity ( $u$ ) normalised by the inlet velocity  $u_{inlet}$ . And the  $y$ -axis is the distance from the symmetric line of the fluid channel normalised by  $h$ . The normalised velocity at the interface is 0.751 for the case of  $\alpha = 0.1$  and the normalised velocity at the center line is 1.13.

Figure 4-6 show the velocity profiles at the outlet of the CFD model for the cases of  $\alpha = 0.5, \alpha = 1$  and  $\alpha = 4$ , respectively. The normalised velocity at the interface are 0.2327 for the case of  $\alpha = 1$  and 0.0706 for the case of  $\alpha = 4$ . These are consistent with the calculation in Mohais et al. [11]. The maximum velocities for all three cases are found in the center lines.

Generally, the fluid-porous interface velocity decreases when the value of  $\alpha$  increases, while the maximum velocity increases with increasing number of  $\alpha$ .

Another fluid-porous interface model, the conservative interface flux model that is available in ANSYS/CFX, was also tested in this study. For the interface flux boundary, the fluid flux at the interface on the fluid domain side is the same as the fluid flux of velocity at the interface on the porous domain. Figure 7 shows the predicted velocity profile using the conservative interface flux model for the fluid-porous interface.

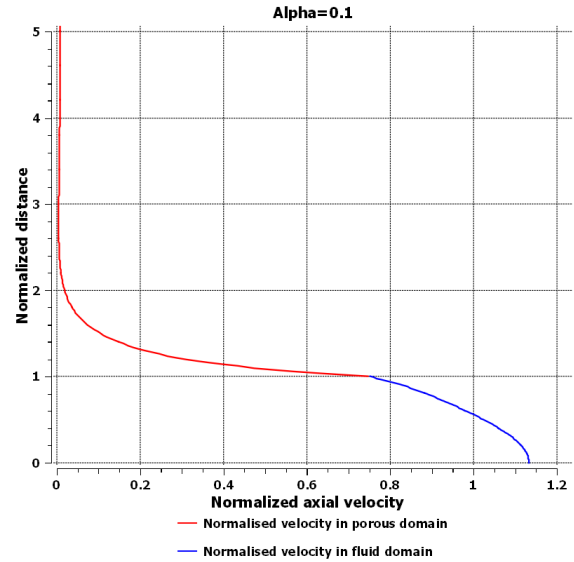


Fig.3. Velocity profile at the outlet for the case of  $\alpha = 0.1$ .

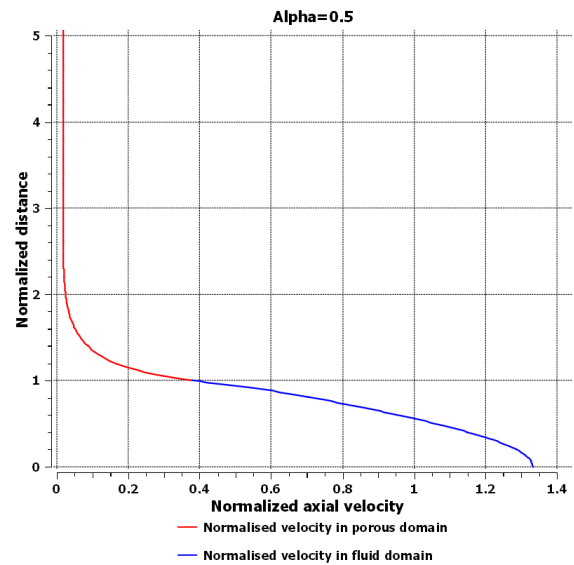


Fig.4. Velocity profile at the outlet for the case of  $\alpha = 0.5$ .

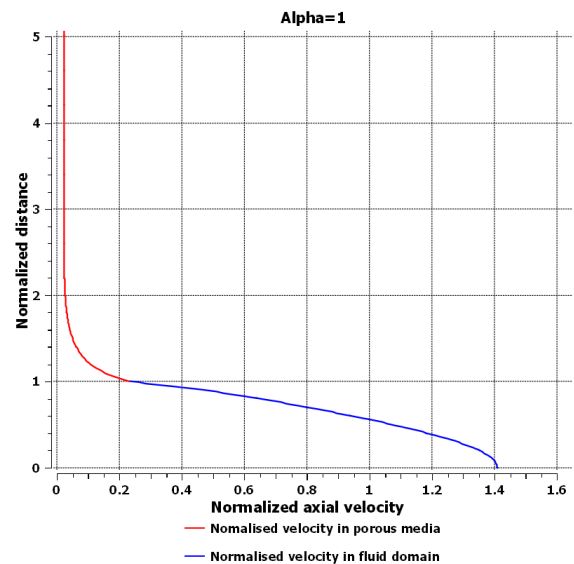


Fig.5. Velocity profile at the outlet for the case of  $\alpha = 1$ .

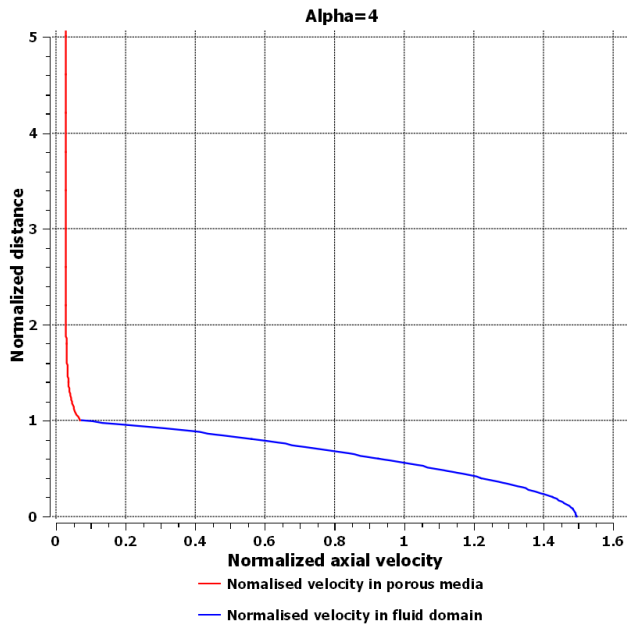


Fig.6. Velocity profile at the outlet for the case of  $\alpha = 4$ .

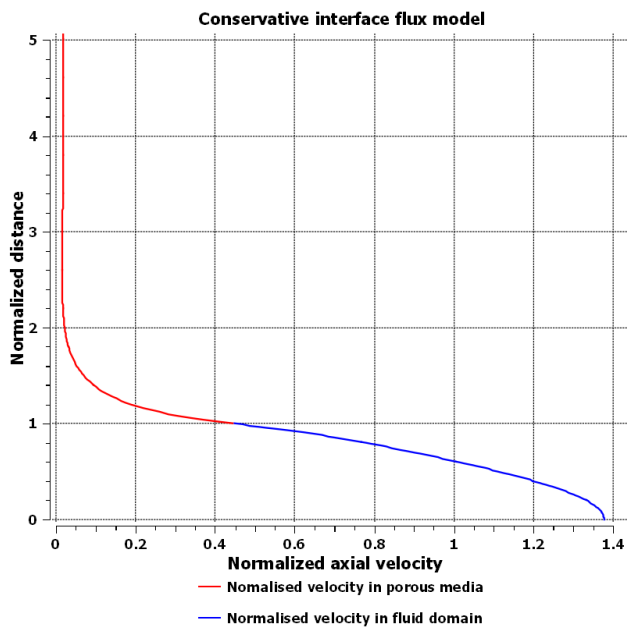


Fig.7. Velocity profile at the outlet for the case of conservative interface flux model.

## Conclusion and future work

The analytical equation of fluid velocity at the fluid-porous interface in a channel fracture developed by Mohais et al. [11] has been implemented in ANSYS/CFX 14.0. One advantage of this model is that it can take into consideration different values of the slip coefficient,  $\alpha$ , which is depending on the porous material.

This fluid-porous interface velocity model has been used to predict the fluid velocity profile in a 2D channel flow in a fluid-porous domain to investigate the effects of values of  $\alpha$  on the flow. Generally, when  $\alpha$  increases from 0.1 to 4, there is an increase in the pressure drop in the flow. The interface velocity decreases and the maximum velocity at the center line of the channel increases as  $\alpha$  increases.

Further investigation of the effect of wall stress on predicted velocity profiles is ongoing.

## Acknowledgements

The work described here was funded by Australian Research Council Discovery Project grant DP110104766.

## References

- [1] Bear, J., *Dynamics of Fluids in Porous Media* New York, Dover Publications, 1988.
- [2] Beavers, G.S. & Joseph, D.D., Boundary conditions at a naturally permeable wall, *J. Fluid Mech.*, **30**, 1967, 197–207.
- [3] Berman, A. S, Laminar flow in channels with porous walls, *J. Appl. Phys.*, **24**, 1969, 1232–1235.
- [4] Breugem, W.P. Boersma, B.J. & Uittenbogaard, R.E., The laminar boundary layer over a permeable wall, *Transp Porous Med.*, **59**, 2005, 267-300.
- [5] Deng, C. & Martinez, D.M., Viscous flow in a channel partially filled with a porous medium and with wall suction, *Chem. Eng. Sci.*, **60**, 2005, 329-336 .
- [6] Enhanced geothermal systems, *Geothermal technologies program*, viewed, 25th may 2012, U.S. Department of ENERGY, [http://www1.eere.energy.gov/geothermal/enhanced\\_geothermal\\_systems.html](http://www1.eere.energy.gov/geothermal/enhanced_geothermal_systems.html).
- [7] Goharzadeh, A., Khalili, A., & Jorgensen, B.B., Transition layer thickness at a fluid porous interface, *Phys. Fluids*, **17**, 2005,057102
- [8] Granger, J. Dodds, J. & Midoux, N., Laminar-flow in channels with porous walls, *Chem Eng J.*, **42**, 1989,193-204.
- [9] Larson, R. E. & Higdon, J. J. L, Microscopic flow near the surface of two-dimensional porous media. Part 2., Transverse flow, *J. Fluid Mech.*, **178**, 1987, 119–136.
- [10] Larson, R. E. & Higdon, J. J. L, Microscopic flow near the surface of two-dimensional porous media. Part 1., Axial flow, *J. Fluid Mech.*, **166**, 1986, 449–472.
- [11] Mohais, R., Xu, C.& Dowd, P.A., An analytical model of coupled fluid flow and heat transfer through a fracture with permeable walls in an EGS, in *proceedings of the 2011 Australian Geothermal Energy Conference*, Department of Resources, Energy and Tourism & Geoscience Australia , Melbourne, Victoria, 2011, 175-179.
- [12] Natarajan, N. & Suresh Kumar, G., Evolution of fracture permeability due to co-colloidal bacterial transport in a coupled fracture-skin-matrix system, *Geoscience Frontiers*, **3**, 2012, 503-514.
- [13] Saffman, P. G., On the boundary condition at the surface of a porous medium, *Studies Appl. Mech.*, **1**, 1971, 93–101.
- [14] Sahraoui, M. & Kaviany, M., Slip and no-slip velocity boundary conditions at inter-face of porous, plain media, *Int. J. Heat Mass Transfer*, **35**, 1992, 927–943.
- [15] Tan, H. & Pillai, K.M. Finite element implementation of stress-jump and stress-continuity conditions at porous-medium, clear-fluid interface, *Comput Fluids*, **38**, 2009, 1118-1131.